R. G. Kirk
Senior Analyst,
Ingersoll-Rand Co.,
Turbo Division,
Phillipsburg, N. J.
Assoc. Mem. ASME

E. J. Gunter
Professor of Mechanical Engineering,
Univ. of Virginia,
Charlottesville, Va.
Mem. ASME

Short Bearing Analysis Applied to Rotor Dynamics

Part 2: Results of Journal Bearing Response

The results of an extensive investigation of the transient response of rotors supported in fluid-film journal bearings is presented in the form of computer generated orbits of rotor motion. The stability of the rotor-bearing system was determined by examination of the system characteristic equation in Part 1. Rotor transient response orbits demonstrate the rotor behavior below and above the stability threshold. The results show the effect of imbalance, steady loading, cyclic unidirectional and rotating loads upon the stability and performance of a short journal bearing. The results are compared to previous investigations and modified stability maps are deduced from the results obtained. The concept of whirl is examined and several plots presented of the instantaneous whirl ratio and radius of curvature versus cycles of motion (of the journal) for the various cases considered. Bearing forces are analyzed and the resulting plots of force versus cycles of motion are presented for selected cases.

Introduction

The derivation of Reynolds equation in Part 1 [1][1] was based on the following standard assumptions:

1 The flow was laminar everywhere in the fluid.

2 The shear stress was related to the shear rate by the viscosity of the fluid (Newtonian fluid) which is constant across the film.

3 Body forces were neglected (i.e., weight of fluid in the film is small in comparison to the other forces acting there).

4 The inertia forces were neglected due to the modified Reynolds number being much less than unity, $\rho UL/\mu\ [h/L]^2 \ll 1$.

5 The pressure across the film was constant.

6 The density of the fluid was a constant.

Reynolds equation for the plane slider bearing was then modified for the journal bearing configuration in rotating coordinates by considering the linear combinations of the effects of rotation, radial motion, and precession. Reynolds equation was derived for the journal bearing in fixed x-y coordinates by expressing unit vectors and reducing the tangential velocities to the fixed coordinate set. In so doing the small angle assumption was used to express sine and tangents as their radian value. The journal bearing equation was then reduced to the short bearing equation by neglecting the radial flow due to pressure gradients; this required the restriction that L/D be less than unity, as verified by Fig. 6 of Part 1.

The equations of motion for the journal were next derived by considering Newton's second law. Gyroscopic effects, angular acceleration, or shaft misalignment was not accounted for and therefore the equations of motion reduced to two coupled, second-order nonlinear differential equations. These equations were then solved by numerical methods for the resulting transient journal motion and form the basis for the following discussion.

Derivation and Explanation of Terms Used in Journal Bearing Studies

As the theory of lubrication has developed, several important equations and groupings of terms have evolved that are used frequently in the field. One of the basic assumptions that has been used in the derivation of the Reynolds equation arose from considering the ratio of inertia to viscous forces in the incompressible Navier-Stokes equation:

$$\rho\frac{\mathrm{Du}}{Dt} = -\nabla p + \mu\nabla^2 u \tag{1}$$

Considering the x direction, the result is

$$\mathrm{Re}^* = \frac{\text{inertia}}{\text{viscous}} = \rho\frac{U^2}{L}\Big/\mu\frac{U}{h^2} = \frac{UL}{\nu}\left(\frac{h}{L}\right)^2 \tag{2}$$

where

Re^* = modified (reduced) Reynolds number
U = velocity
L = characteristic length

[1] Numbers in brackets designate References at end of paper.

Contributed by the Lubrication Division of THE AMERICAN SOCIETY OF MECHANICAL ENGINEERS and presented at the Lubrication Conference, Miami Beach, Fla., October 21–23, 1975. Manuscript received at ASME Headquarters, July 16, 1975. Paper No. 75-Lub-31.
Copies will be available until July, 1976.

h = film thickness
ν = kinematic viscosity

The distinction has been made to call this expression a modified Reynolds number since the expression frequently used as the Reynolds number in fluid mechanics work is given as: Re = UL/ν.

From this relation it is seen that

$$\mathrm{Re}^* = \mathrm{Re} \times \left(\frac{h}{L}\right)^2. \tag{3}$$

Another much used expression known as Sommerfeld's number resulted from the work of Sommerfeld [2] in 1904 when he presented the exact solution to the long bearing assumption form of Reynolds equation. The result of this work was an expression for the loading of an idealized full journal bearing. The result can be expressed as follows [3]:

$$\left(\frac{r}{c}\right)^2 \frac{\mu N'}{P} = \frac{(2+\epsilon^2)\sqrt{1-\epsilon^2}}{12\,\pi^2\epsilon} \tag{4}$$

where

N' = journal speed (rps)
ϵ = eccentricity = e/c
r = journal radius = R
P = load per area of the projected area of journal = $W/(L \times D)$, $D = 2R$

The expression

$$\frac{\mu N'}{P}\left(\frac{R}{c}\right)^2 \tag{5}$$

is known as Sommerfeld's number (S).

An equivalent expression can be derived for the short-bearing assumption form of Reynolds equaion. Using polar coordinates and making use of certain integral formulas due to Sommerfeld, it is possible to successfully integrate Reynolds equation to obtain the load capaciy. This result can be expressed by

$$\mathrm{S_S} = \frac{\mu N'}{P}\left(\frac{L}{2c}\right)^2 = S\left(\frac{L}{D}\right)^2 = \frac{(1-\epsilon)^2}{\pi\epsilon[\pi^2(1-\epsilon^2)+16\epsilon^2]^{1/2}} \tag{6}$$

The same expression has been derived by Ocvirk [5] and is referred to as the "capacity number" for the bearing inthat report (see Fig. 1).

The attitude ϕ can be found by forming the ratio of the tangential and radial load components, the result of which is given by [4]:

$$\tan\phi = \frac{\pi}{4}\frac{(1-\epsilon^2)^{1/2}}{\epsilon} \tag{7}$$

The value of P, the projected load, is usually considered as the effective journal weight divided by the product of length and diameter of the bearing. When considering imbalance loading effects it may be helpful to form the Sommerfeld number based on the rotating load. In doing this, P becomes the quantity $me_\mu\omega^2$, the magnitude of the unbalance loading. The resulting expression is

$$S_U = \frac{\mu N'}{P_U}\left(\frac{R}{c}\right)^2 \tag{8}$$

where

$P_U = (me_\mu\omega_j^2)/(L \times D)$
S_U = Sommerfeld number for unbalance loading

The stability plots for journal bearings that appear in the literature are usually plotted with a dimensionless speed parameter as ordinate and eccentricity ratio, ϵ, as abscissa. The speed parameter may be thought of as the square root of the ratio of the unbalance force (with $e_\mu = c$) to the journal weight. That is

$$\omega_S = \sqrt{mc\omega_j^2/mg} \tag{9}$$

or

$$\omega_S = \omega_j/\sqrt{g/c} \tag{10}$$

where $\sqrt{g/c}$ has units of s^{-1} and, as stated previously, makes the speed parameter dimensionless.

An important consideration when designing bearings is the magnitude of the actual forces transmitted to the bearing surface.

This quantity can be calculated from equation (28) of Part 1 and could be represented as

$$\hat{F} = \sqrt{F_x^2 + F_y^2} \tag{11}$$

where F_x, F_y = magnitude of fluid-film forces in the x and y coordinate directions, respectively.

It is possible now to form two dimensionless force parameters, to be denoted as static and dynamic transmissibility, given by

$$TR_S = \hat{F}/W \tag{12}$$

and

Nomenclature

E_0, ES = eccentricity ratio calculated using the total resultant journal load for P in the Sommerfeld equation
E_μ, EMU = unbalance eccentricity ratio = e_μ/c
EN = ratio of rotating load angular speed = ω_{F0}/ω_j
ENX = ratio of oscillating horizjntal load angular speed = ω_{FHX}/ω_j
ENY = ratio of oscillating vertical load angular speed = ω_{FHY}/ω_j
ESU = eccentricity calculated using unbalance load as loading force
e = radial journal center displacement, L
e_μ = unbalance eccentricity, L
FHX = magnitude of horizontal oscillating load (x direction), F
FHY = magnitude of vertical (y direction) oscillating load, F
$FMAX$ = maximum fluid film force developed per run, F
FU = magnitude of unbalance load, F
$FURATIO$ = ratio of unbalance load to journal weight
FX, FY = constant load on journal in the x and y coordinate directions, respectively, F
g = acceleration of gravity = 386, L/T^2
H = dimensionless film thickness = h/c
h = film thickness, L
i, j, k = unit vectors in the fixed x-y-z coordinate directions
MU = viscosity of fluid film, F-T/L^2
S = Sommerfeld number = $\mu N/P\ (R/c)^2$, rev
SS, S_S = short bearing Sommerfeld number (capacity number, Ocvirk number) = $S \times (L/D)^2$, rev
SU, S_U = Sommerfeld number based on the unbalance loading, where $P = P_U$, rev
T = dimensionless time = $\omega_j t$
TR = transmissibility
TR_D = dynamic transmissibility = $m_j e_\mu \omega_j^2/W$
TR_S = static transmissibility = F/W
$TRDMAX$ = maximum value of TR_D
$TRSMAX$ = maximum value of TR_S
W = effective weight of the journal, F
WS = speed parameter = $\sqrt{m_j c\omega_j^2/W_T}$
W_T = total constant load on journal, F
WT = ratio of total constant load to journal effective weight = W_T/W
β = phase angle between the journal displacement vector and the unbalance eccentricity vector, deg
ϵ, ϵ_0 = eccentricity ratio = e/c
ϵ_0 = eccentricity calculated from equation of S_S
η = ratio of rotating load velocities = ω_{F0}/ω_j
μ = viscosity, F-T/L^2
ν = kinematic viscosity, = μ/ρ, L^2/T
ρ = density, F-T^2/L^4
Ω, ω_j = journal angular velocity, T^{-1}
Ω_S = speed parameter, = $\omega_j/\sqrt{W_T/m_j c}$
ω_b = bearing angular velocity, T^{-1}
ω = speed parameter = $\omega_j/\sqrt{g/c}$, T^{-1}

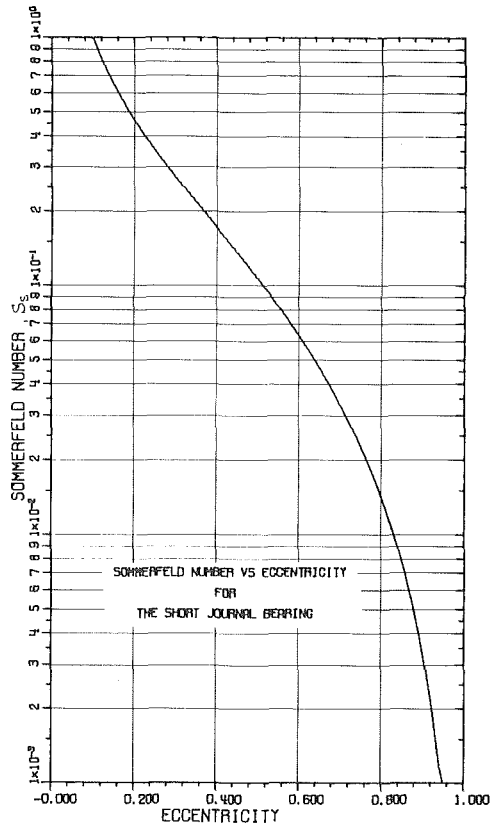

Fig. 1 Sommerfeld number versus eccentricity for the short journal bearing

$$TR_D = \hat{F}/(me_\mu \omega_j^2) \tag{13}$$

These ratios give an indication of the isolation of the journal from the support system. A value of 1 is equivalent to a system on rigid ball bearing supports, whereas for $TR < 1$, there is an improvement of performance due to lower forces transmitted. If $TR > 1$, then the journal bearings are actually developing higher forces than if the system were mounted in rigid ball bearings. This latter mode of operation is not desirable and should be avoided by the designer. If this is not possible, the transmissibility should be reduced to the lowest value attainable.

Presentation of Results

The methods of solution incorporated in the computer program developed from the theory of Part 1 were chosen such that the investigator had the choice of

(a) rapid solution and reasonable accuracy (improved Euler's method),

(b) reasonable speed of solution and improved accuracy (modified Adam's method), but with the problem of numerical instability greatly increased over (a),

(c) excellent accuracy and less instability than (b) but very time consuming (sixth-order Runge-Kutta method).

Many runs have been made with the program and an extensive file of different operating conditions was compiled. The following results were chosen to give a general presentation of the various results which have been obtained. The basic journal bearing under consideration has the following specifications:

Journal weight—22.68 kg (50 lb)
Clearance—0.0127 cm (0.005 in.)
Diameter—5.08 cm (2.0 in.)
Length—2.54 cm (1.0 in.)
Viscosity of lubricant—68.97 cp (1.0×10^{-5} reyns)
Imbalance—variable
Loading—variable
Journal speed—variable

Modified specifications are used to help clarify the different concepts being discussed and also to demonstrate the flexibility of the developed program.

The stability of a horizontal balanced journal is considered initially and results in a modification of the stability map discussed previously in Part 1. The last section will take into consideration the effect of imbalance and other cyclic external loading functions on the overall journal bearing performance.

Instability of Horizontal Balanced Journal Bearings

For the purpose of this discussion, a horizontal bearing is one having the journal effective weight acting at right angles to the axial coordinate of the journal. Fig. 2(a) shows the orbit of the 22.68 kg (50 lb) journal as it is started at the bearing center while operating at a speed of 66.67 Hz (4000 rpm). Five cycles of motion are shown in the figure and it is obvious that the journal has settled to the equilibrium eccentricity of 0.306 as computed from the bearing capacity number and indicated as ES on the figure. The maximum force transmitted to the bearing is indicated by FMAX and is recorded as 261.1N (58.7 lb) and occurs 0.29 cycles after the journal was released. By checking the speed parameter, WS, and the eccentricity on the stability map (Fig. 14 of Part 1) it is apparent that the system is operating in a stable region as predicted by the stability map.

The transmissibility, TR, is plotted for this case in Fig. 2(b) (the solid line). Notice that the TR factor levels off to a value of 1 after about three cycles of motion. The dashed lines on this plot give the X and Y motion versus cycles of journal motion as indicated. Fig. 2(c) shows the instantaneous whirl ratio and radius of curvature for this case. The radius reduces to zero as it should while the whirl is oscillating in a very regular manner. Constant whirl ratios have been reported to exist in test rigs but it will be apparent from the following discussion and figures that this is a misnomer for the horizontal bearing.

The next series of plots (Figs. 3(a), 3(b)) represents the previous case with the speed increased to 108.3 Hz (6500 rpm). A different behavior is immediately noticed and by checking the stability map

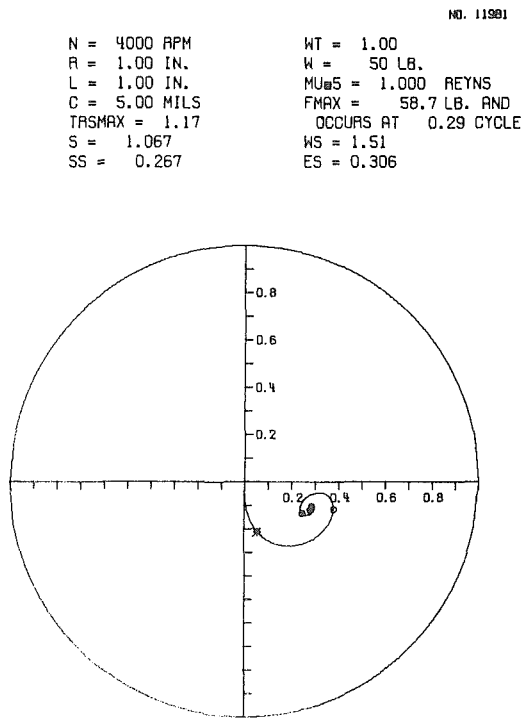

Fig. 2(a) Journal orbit of a balanced horizontal rotor (N = 66.67 Hz., W = 22.68 kg, C = 0.0127 cm, L/D = ½)

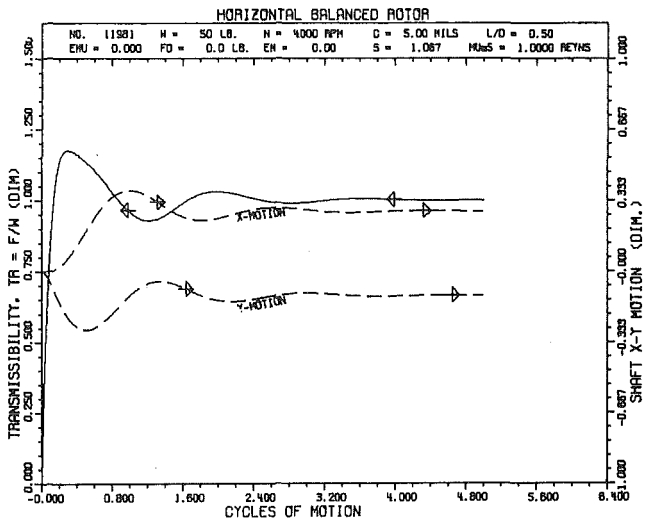

Fig. 2(*b*) Transmissibility and shaft *X-Y* motion versus cycles of motion (*N* = 66.67 Hz)

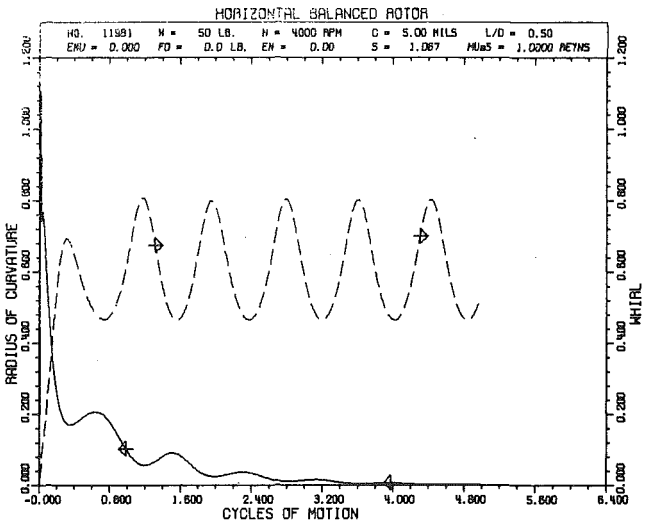

Fig. 2(*c*) Radius of curvature and whirl versus cycles of motion (*N* = 66.67 Hz)

it is apparent that the system is operating on the threshold of instability by the values given for *WS* and *ES*. The maximum force has increased to 286.5N (64.4 lb). From Fig. 3(*b*), the whirl is varying from a value of 0.44 up to a value about 0.64. The timing circles on the orbit of Fig. 3(*a*) are indicative of an average whirl of approximately one-half.

If the journal speed were now increased to 175 Hz (10,500 rpm) the speed parameter, *WS*, would be 3.96 and well into the region of instability. Fig. 4(*a*) shows this condition with the final position in Fig. 3(*a*) as the initial condition for this plot. The spiral is evidence of the instability of the system and if more cycles were run the orbit would reach a limit cycle and continue the violent whirling motion. It is apparent that the rate of growth of the orbit has reduced and a limit cycle would eventually be formed. The maximum force has increased to a value of 880.3N (197.9 lb). The whirl ratio is oscillating around approximately 0.5, as shown in Fig. 4(*b*).

Fig. 5(*a*) depicts the initial transient orbit for a heavier journal with an effective weight of 90.72 kg (200 lb) and operating at 108.3 Hz (6500 rpm). This case is still at the threshold of stability although the equilibrium eccentricity has increased to 0.497. An increase of journal speed to 175 Hz (10,500 rpm) raises the stability speed parameter to 3.96 and the system exhibits the predicted in-

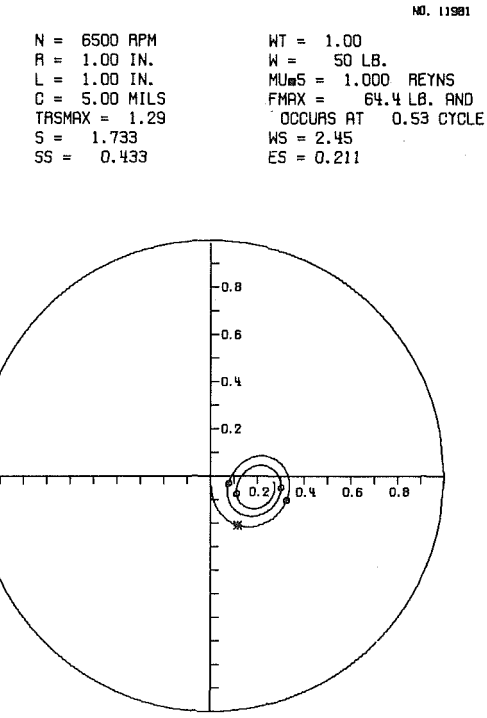

Fig. 3(*a*) Journal orbit of a balanced horizontal rotor (*N* = 108.3 Hz, *W* = 22.68 kg, *C* = 0.0127 cm, *L/D* = ½)

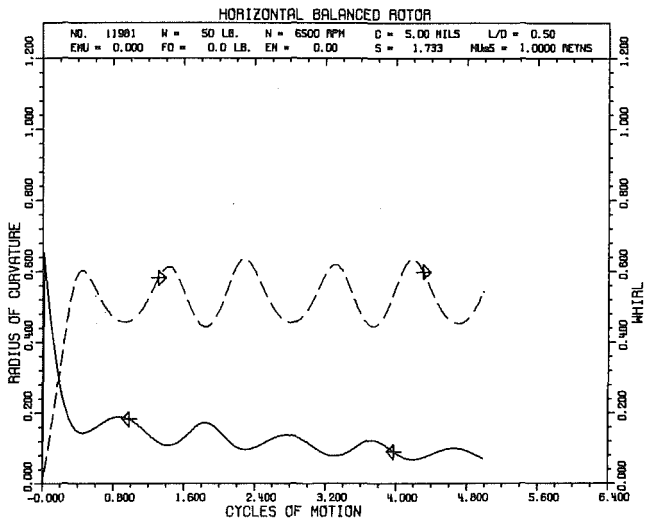

Fig. 3(*b*) Radius of curvature and whirl versus cycles of motion (*N* = 108.3 Hz)

stability as shown in Fig. 5(*b*). The maximum force is indicated to be 3677.8N (826.8 lb) or 4.13 times the weight of the journal.

The stability map predicts that for systems with an equilibrium eccentricity above approximately 0.73, there should exist stable conditions at any speed. With the journal weight increased to 816.48 kg (1800 lb), Figs. 6(*a*) and 6(*b*) indicate that the system is tending toward the stable equilibrium position, even when the speed is increased to 175 Hz (10,500 rpm). The stability map of Part 1 has predicted all the results obtained thus far in this analysis. However, no indication can be obtained from such a stability map of the behavior of a system that has external loading. To examine this condition, a constant force of 667.2N (150 lb) was applied vertically downward (i.e., negative *y* direction) to the 22.68 kg (50 lb) journal to see if the conditions of the 90.72 kg (200 lb)

journal were repeated. Fig. 7 gives the interesting results of that loading. The journal has settled very smoothly into its equilibrium eccentricity of 0.497. The speed parameter corresponding to Fig. 14 of Part 1 is still 2.45 and indicates that the system should be at its threshold speed. An increase of journal speed to 175 Hz (10,500 rpm) should produce violent whirling if Fig. 14 is valid. It is readily apparent from Fig. 8 that the system is stable at 175 Hz (10,500 rpm) and has settled very nicely into the new equilibrium eccentricity of 0.395. In response to these results, Fig. 14 has been modified to indicate the stability of a journal bearing with constant external loading.

If a new speed parameter is defined as

$$\Omega_S = \omega_j/\sqrt{W_T/(mjc)}$$

where

W_T = total loading

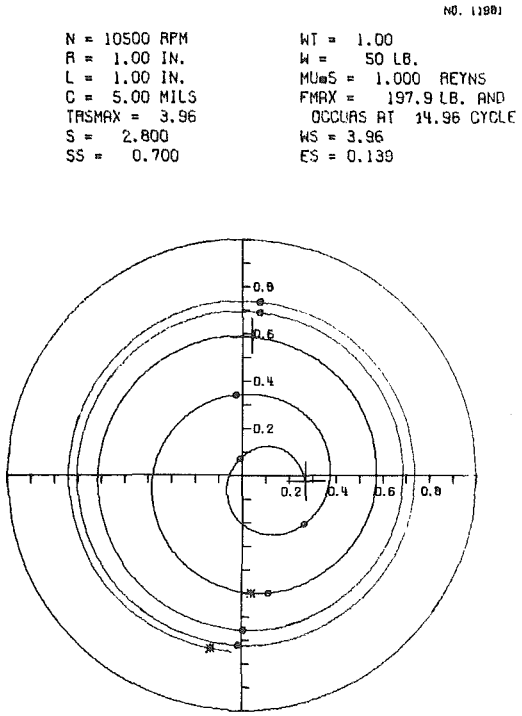

Fig. 4(*a*) Journal orbit of a balanced horizontal rotor for cycles 5–15 (N = 175 Hz, W = 22.68 kg, C = 0.0127 cm, L/D = ½)

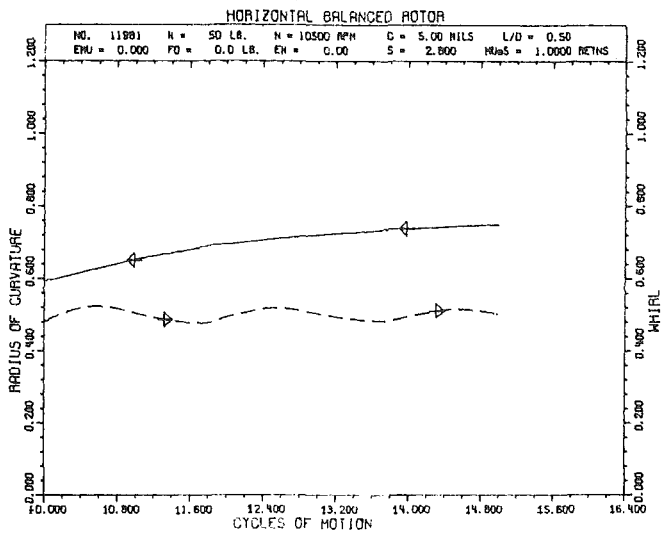

Fig. 4(*b*) Radius of curvature and whirl versus cycles of motion for cycles 10–15 (N = 175 Hz)

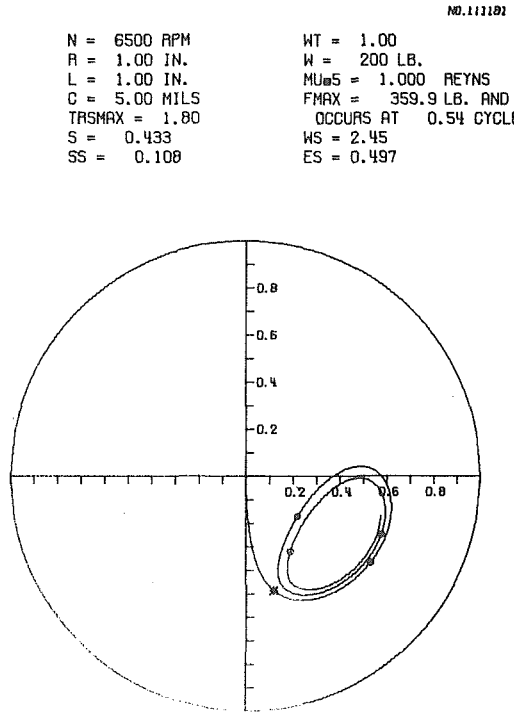

Fig. 5(*a*) Journal orbit of a balanced horizontal rotor for 5 cycles (N = 108.3 Hz, W = 90.72 kg, C = 0.0127 cm, L/D = ½)

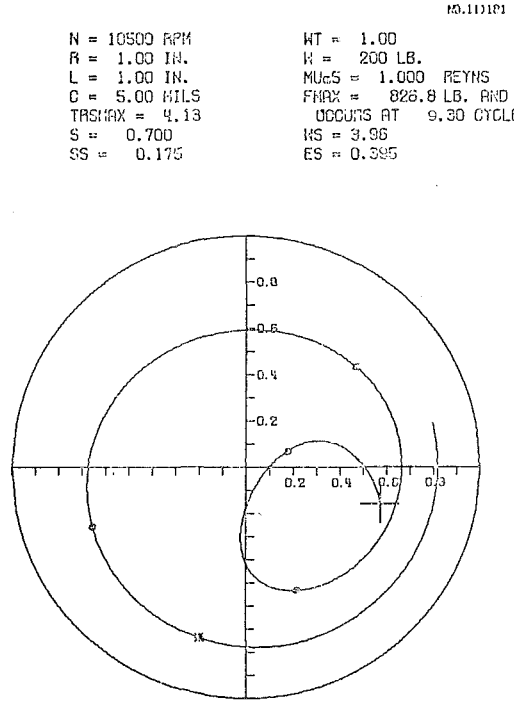

Fig. 5(*b*) Journal orbit of a balanced horizontal rotor for cycles 5–15 (N = 175 Hz)

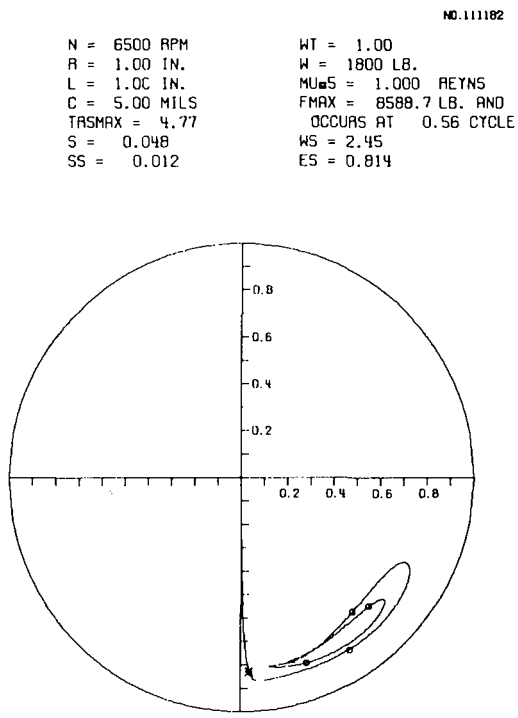

Fig. 6(*a*) Journal orbit of a balanced horizontal rotor for 5 cycles (*N* = 108.3 Hz, *W* = 816.48 kg, *C* = 0.0127 cm, *L/D* = ½)

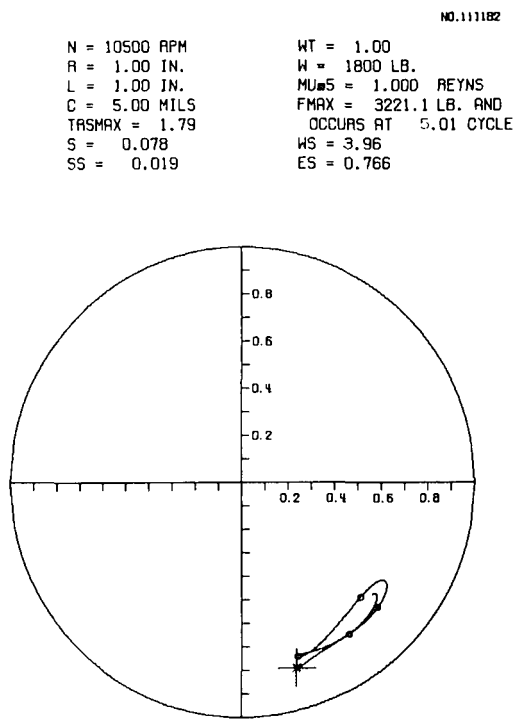

Fig. 6(*b*) Journal orbit of a balanced horizontal rotor for 5–10 cycles (*N* = 108.3 Hz, *W* = 816.48 kg, *C* = 0.0127 cm, *L/D* = ½)

and E_0 = eccentricity of journal calculated by using W_T instead of W in the projected load, P, of the Sommerfeld equation (S_s) then the stability map of Fig. 9 may be obtained. By redefining the speed parameter and using the actual value of equilibrium eccentricity, then and only then can the curve of Fig. 14 of Part 1 be considered as correct for other than unloaded bearings.

The Horizontal Journal With Imbalance

Fig. 10(a) represents the behavior of a horizontal 22.68 kg (50 lb) journal operating at 108.3 Hz (6500 rpm). Due to the gravity

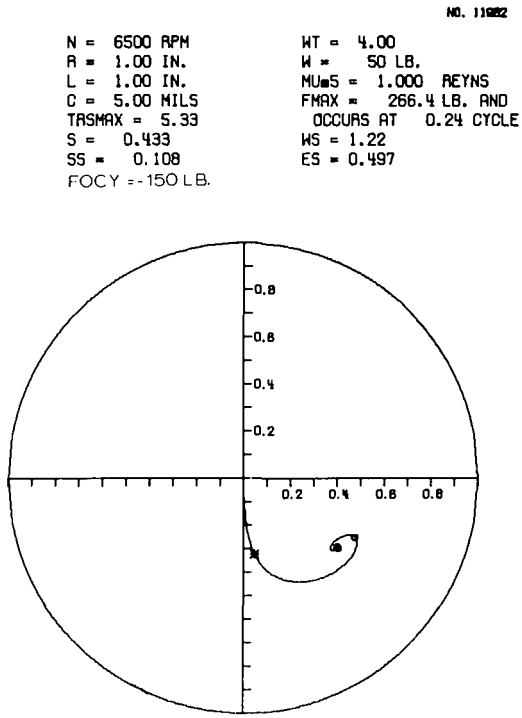

Fig. 7 Journal orbit of a horizontal balanced rotor with constant load for 5 cycles (*N* = 108.3 Hz, *W* = 22.68 kg, *C* = 0.0127 cm, *L/D* = ½, *FOCY* = −667.26N)

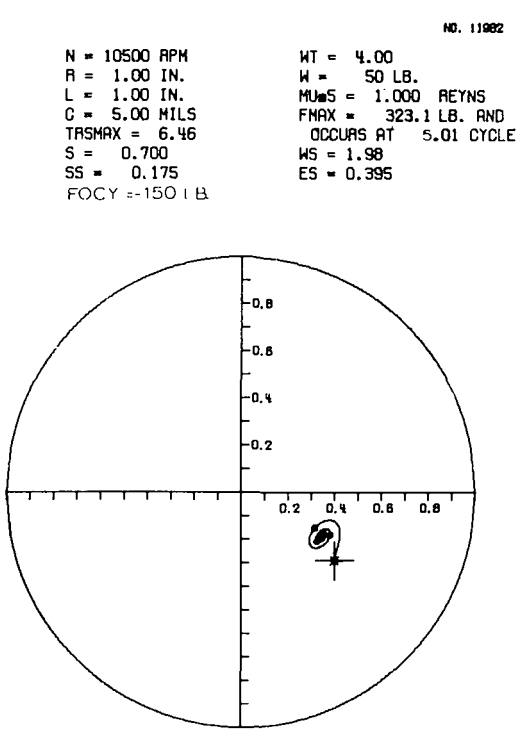

Fig. 8 Journal orbit of a horizontal rotor with constant load for cycles 5–10 (*N* = 175 Hz)

loading, the orbit is displaced by the steady-state eccentricity ES = 0.21. The nonsynchronous component is less than one-half due to the inner loop precessing in a counterclockwise direction. The imbalance load is 266.7N (59.95 lb) as indicated by FU. The TR factor was observed to be oscillating between a value of almost zero and up to a maximum of about 2.3. This is approximately twice the value obtained with a vertical rotor. The oscillation of the loading on the bearing could considerably reduce the life of the bearing due to fatigue failure of the bearing surface.

Fig. 10(*b*) shows five additional cycles of motion at the speed of 175 Hz (10,500 rpm). A limit cycle is forming but the component of displacement due to the synchronous imbalance forcng function is still affecting the resultant orbit in this case. The fact that the inflections are moving counterclockwise indicates that the nonsynchronous component is less than one-half the journal speed.

An increase of *EMU* to a value of 0.8 produces the "synchronous" limit cycle of Fig. 11(*a*). Figs. 11(*b*), 11(*c*), and 11(*d*) are the transmissibility, whirl ratio, radius, and phase angle plots for this case.

Note the cyclic nature of the forces on the bearing as indicated by the *TR* plot and the fact that the whirl is oscillating about the value of 1.0 while the timing marks on the orbit plot are coming on top of each other and make it appear that the orbit is abolute synchronous while it is not.

With an increase of speed to 175 Hz (10,500 rpm) the limit cycle grows accordingly as shown in Fig. 12(*a*) and the synchronous forcing function predominates the resultant orbit motion. The radius and whirl plot for this case is included as Fig. 12(*b*) and concludes the series of figures being presented which are related to imbalance loading alone.

The cases presented have shown that imbalance in a horizontal rotor will increase the forces being transmitted to the bearings and therefore should be reduced to the smallest value possible. No advantage, as was found for the vertical journal [9], can be had from imbalance in a horizontal rotor.

Motion of a Journal Bearing Experiencing Cyclic External Loading

A journal bearing in actual use must support the journal and rotor system and in addition it must be able to maintain its stability and load-carrying capacity under any type of external loading that might occur. For example, the main bearings of an internal combustion engine experience severe cyclic loading functions through the connecting rods. Journal bearings must be able to support shock loading, plane cyclic loading, rotating loads other than imbalance, or any other type loading that a particular application might involve.

The following sample cases were chosen to illustrate the ability of the method of solution to produce the resulting journal orbits.

Fig. 13(*a*) indicates the orbit of a 90.72 kg (200 lb) vertical journal with a clearance of 9.55×10^{-3} cm (3.76 mils) operating at 60 Hz (3600 rpm) and experiencing a −889.6N (−200 lb) load that is rotating backward at ½ the journal angular frequency. The resulting "three-bladed propeller" is the resultant motion of a forward

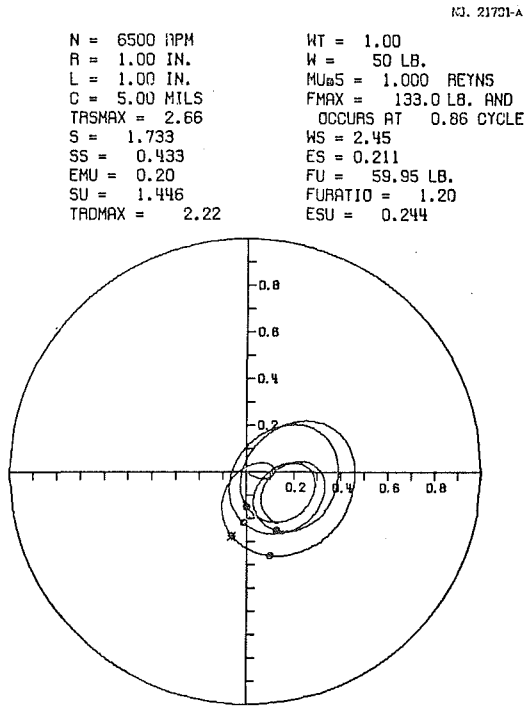

Fig. 10(*a*) Journal orbit of an unbalanced horizontal rotor at the stability threshold for 5 cycles (*N* = 108.3 Hz, *W* = 22.68 kg, *C* = 0.0127 cm, *L/D* = ½, *EMU* = 0.2)

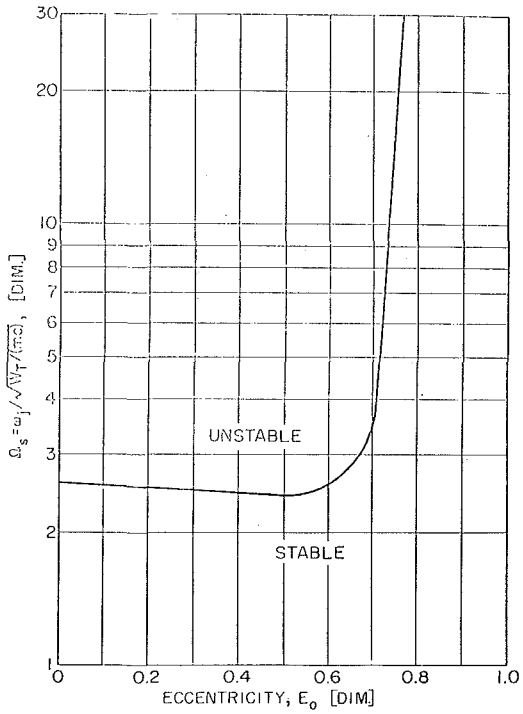

Fig. 9 Stability map for the short journal bearing using modified stability parameters

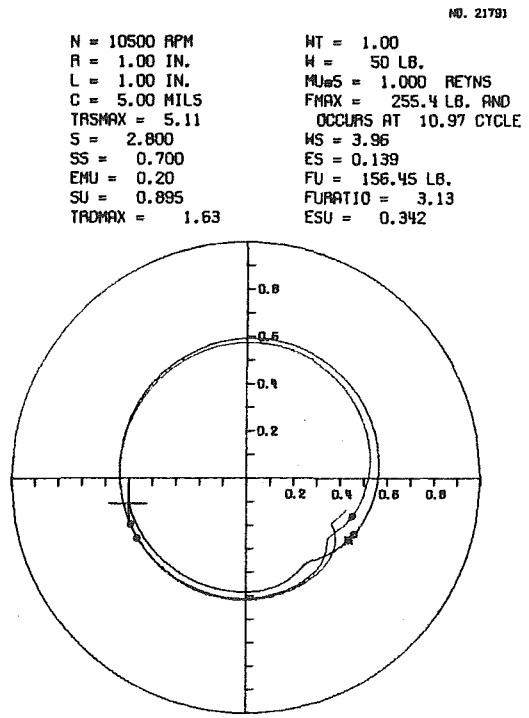

Fig. 10(*b*) Journal orbit of an unbalanced horizontal rotor for cycles 10–15 showing the nonsynchronous limit cycle (*N* = 175 Hz)

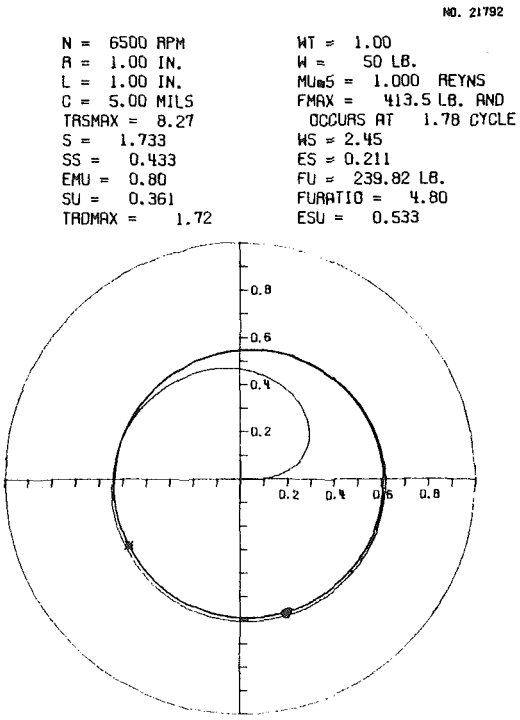

Fig. 11(*a*) Journal orbit of an unbalanced horizontal rotor showing synchronous motion at the stability threshold for 5 cycles (N = 108.3 Hz, W = 22.68 kg, C = 0.0127 cm, L/D = ½, EMU = 0.8)

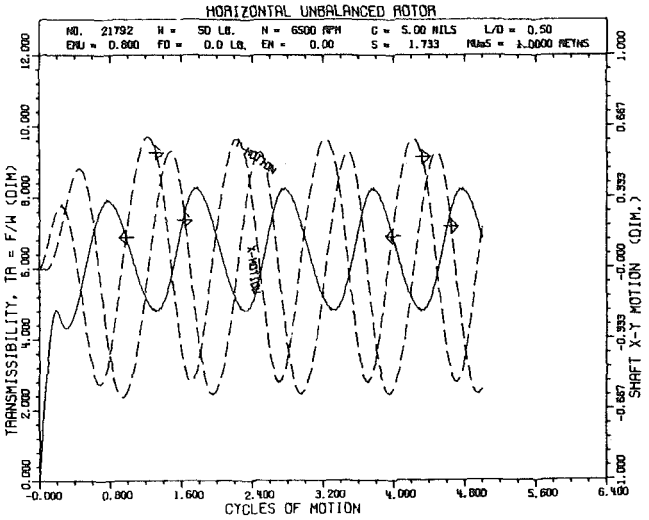

Fig. 11(*b*) Transmissibility and shaft X-Y motion versus cycles of motion (N = 108.3 Hz)

synchronous component plus a nonsynchronous component rotating backward at one-half the angular velocity of the synchronous component.

By applying the formula given by Hull [7] there should have been approximately two outer loops. The difference is, of course, that the imbalance forcing function has altered the effect of the external rotating load and results in the three outer loops of Fig. 13(*a*). This type of motion has actually been observed experimentally with two-pole electric motors supported in plane journal bearings.

The same conditions for a horizontal bearing are shown in Fig. 13(*b*) with the corresponding whirl and curvature plot presented in Fig. 13(*c*).

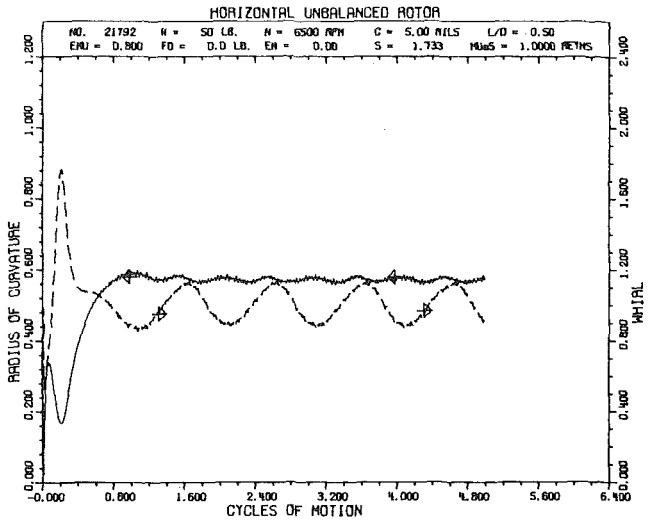

Fig. 11(*c*) Radius of curvature and whirl versus cycles of motion (N = 108.3 Hz)

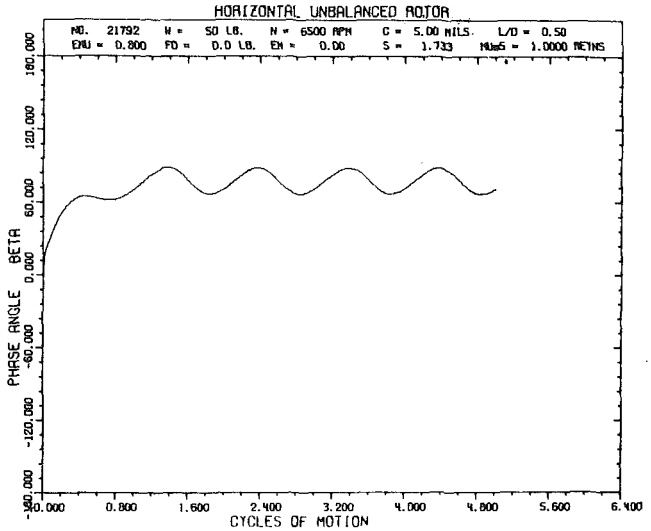

Fig. 11(*d*) Unbalance-displacement phase angle versus cycles of motion (N = 108.3 Hz)

The next three series of figures are for a 22.68 kg (50 lb) journal with a clearance of 0.0127 cm (5 mils) experiencing cyclic loading functions. Each case is allowed to run for five cycles of journal rotation, which is 108.3 Hz (6500 rpm).

The first case, Fig. 14, has a forward rotating load, rotating at one-half the journal speed. A maximum load of about 2224.1N (500 lb) is developed in the bearing after 3½ cycles as indicated on the plot.

The second case, Fig. 15(*a*), is for a 444.8N (100 lb) backward rotating load (EN = −0.5). This case is very similar to that of Fig. 13(*b*) but the synchronous component is not as prevalent so the motion is very close to being backward half-frequency whirl. The instantaneous whirl is given in Fig. 15(*b*) and is oscillating about the −0.5 value.

It is obvious that the direction of rotation of the external load has a great effect on the size of the resulting orbit for the given case of the frequency ratio being ½. From equation (8*a*) of Part 1, it is obvious that the entire wedge effect of the journal bearing is lost if the precession rate, $\dot{\phi}$, is exactly one-half shaft speed. This explains the large limit cycle for the case of the forward rotating load (Fig. 14) as compared to the relatively small orbit for the backward rotating half-frequency load (Fig. 15(*a*)).

The next case (Fig. 16(a)) considered has a vertical (y-coordinate) oscillating load of FHY = 444.8N (100 lb) and the frequency is one-half the journal angular velocity, ω_j. The orbit spirals out in phase with the exciting force and would eventually reach a limit cycle and continue the whipping motion. Fig. 16(b) indicates a mean value of 0.5 for the whirl under these conditions.

It would be impossible to include examples of all variations of the loading functims possible with the present program makeup, not to mention the capability of reading force values from data cards into the program for each increment of dimensionless time, T.

Discussion of Results and Conclusions

This analysis has proven the feasibility of incorporating fixed Cartesian coordinates in the study of journal bearings instead of using the standard rotating coordinates. This makes the extension of a rotor dynamics program to include fluid film bearings very simple since, without doubt, Cartesian coordinates are the standard coordinate set used in rotor-shaft analyses and therefore the extension would not require a transformation between coordinate sets.

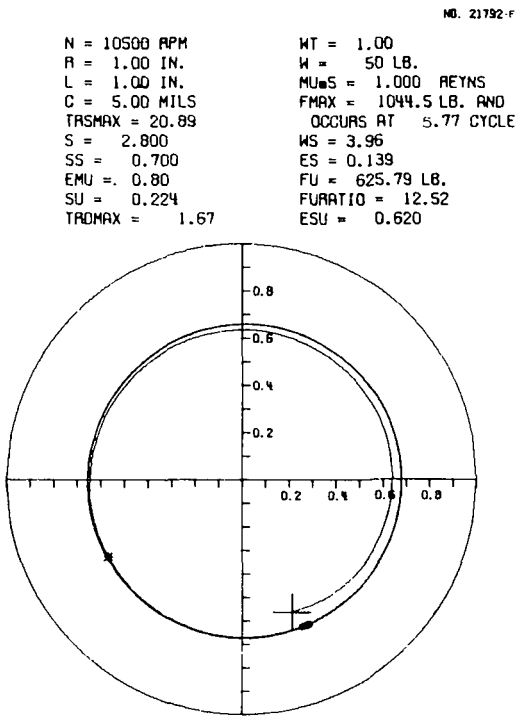

Fig. 12(a) Journal orbit of an unbalanced horizontal rotor above the stability threshold for cycles 5–10 showing synchronous limit cycle (N = 175 Hz)

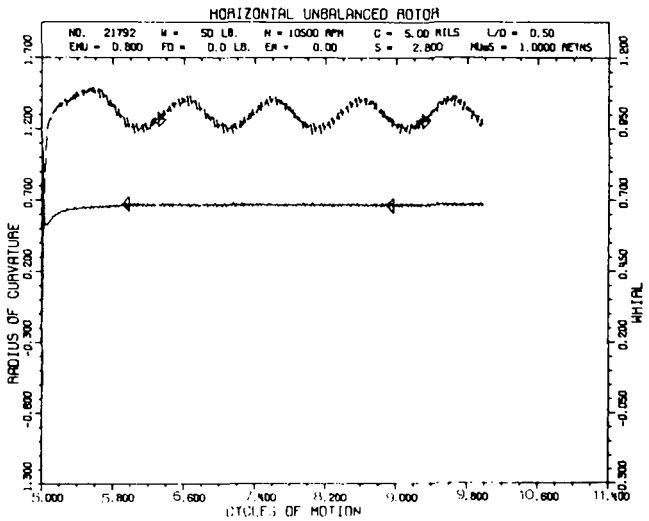

Fig. 12(b) Radius of curvature and whirl versus cycles of motion for cycles 5–10 illustrating small numerical instability (N = 175 Hz)

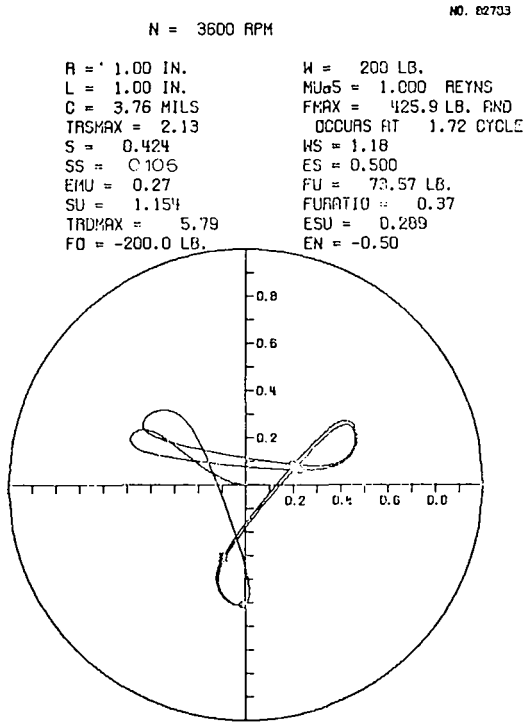

Fig. 13(a) Journal orbit of an unbalanced vertical rotor having a backward half-frequency rotating load for 5 cycles (N = 60 Hz, W = 90.72 kg, C = 0.00955 cm, L/D = ½, FO = −889.3N, EN = −0.5, EMU = 0.27)

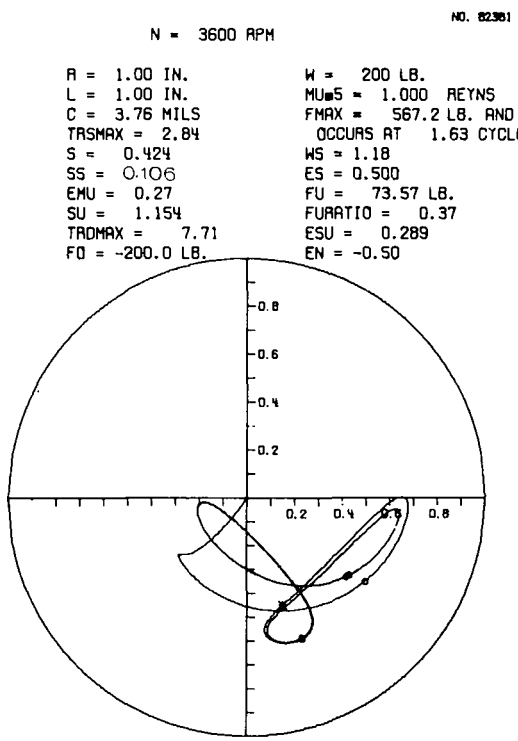

Fig. 13(b) Journal orbit of an unbalanced horizontal rotor having a backward half-frequency rotating load for 5 cycles (N = 60 Hz, W = 90.72 kg, C = 0.00955 cm, L/D = ½, FO = −889.3N, EN = −0.5, EMU = 0.27)

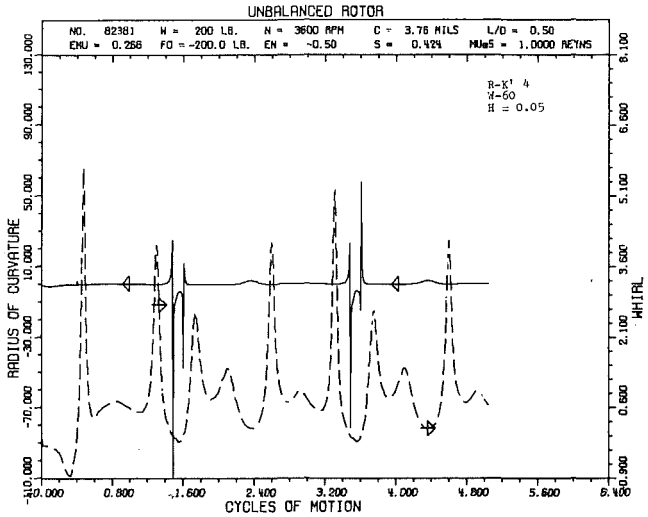

Fig. 13(*c*) Radius of curvature and whirl versus cycles of motion for an unbalanced horizontal rotor (*N* = 60 Hz)

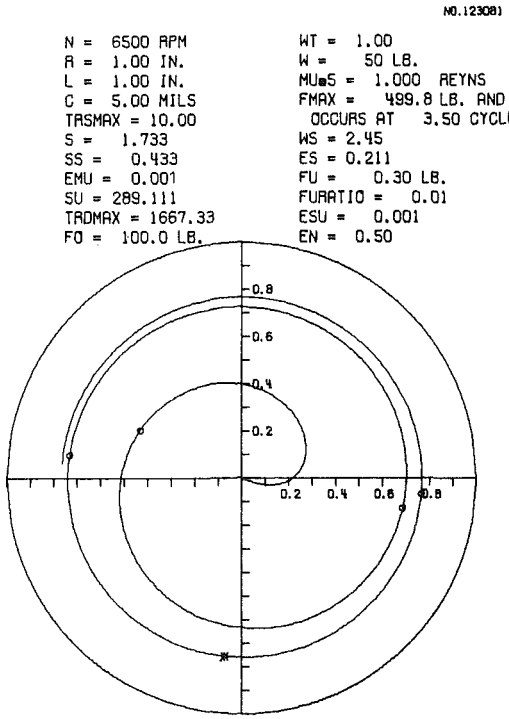

Fig. 14 Journal orbit of an unbalanced horizontal rotor having a forward half-frequency rotating load for 5 cycles (*N* = 108.3 Hz, *W* = 22.68 kg, *C* = 0.0127 cm, *L/D* = ½, *EMU* = 0.001, *FO* = 444.8N, *EN* = −0.5)

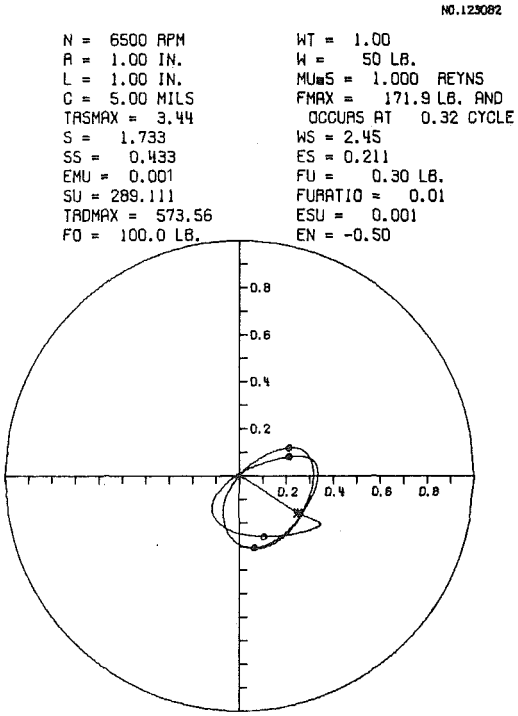

Fig. 15(*a*) Journal orbit of an unbalanced horizontal rotor having a backward half-frequency rotating load for 5 cycles (*N* = 108.3 Hz, *W* = 22.68 kg, *C* = 0.0127 cm, *L/D* = ½, *EMU* = 0.001, *FO* = 444.8N, *EN* = −0.5)

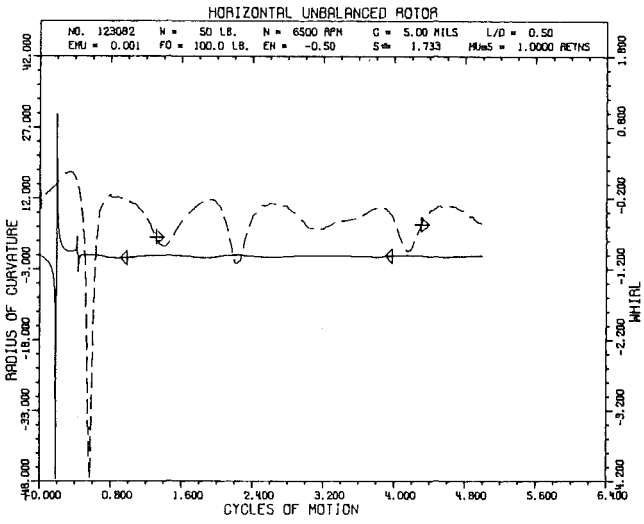

Fig. 15(*b*) Radius of curvature and whirl versus cycles of motion (*FO* = 444.8N, *EN* = 0.5)

The modified stability map presented in Fig. 9 is of great importance when considering the design of journal bearings that are operating under external loading or those that are used for a particular application where the system axial coordinate might be inclined at an angle to the horizontal. Fig. 9 indicates that the region of instability increases at the system is tilted from the horizontal and the balanced vertical unloaded journal is unstable for all speeds of operation.

The constant external loading has been shown to stabilize the journal with far less total load than indicated as necessary by the stability map of Badgley [8] (Fig. 15 of Part 1). The example given in this paper illustrated that a 667.23N (150 lb) external load would stabilize the 22.68 Kg (50 lb) rotor, whereas the stability map of Badgley indicates that the only way to stabilize the system is to increase the equilibrium eccentricity to a value greater than about 0.73, as illustrated by Fig. 6. The system was shown to be very stable at an eccentricity of 0.395 under the external load, as shown in Fig. 8 and predicted by Fig. 9.

The horizontal journal, in all cases tested, did not have the static or dynamic transmissibility below a value of one at any time. Fig. 11(*a*) was the only plot presented of the phase angle between the imbalance and the journal center displacement. Two important conclusions can be obtained from this plot for the imbalanced horizontal rotor. Fig. 11(*a*) shows the resultant synchronous limit cycle of the journal center but the phase angle in Fig. 11(*a*) has a substantial variation in magnitude. Many investigators assume a constant phase angle to reduce the labor involved in obtaining closed-form solutions for less complex rotor simulations. This sin-

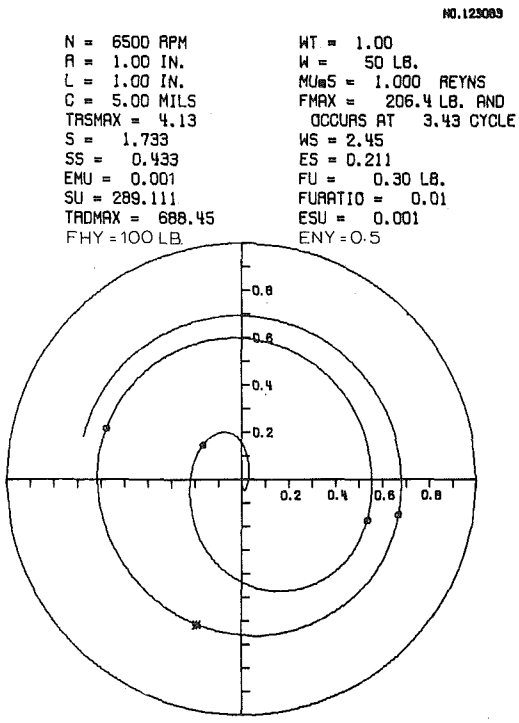

Fig. 16(*a*) Journal orbit of an unbalanced horizontal rotor having unidirectional harmonic loading for 5 cycles (*N* = 108.3 Hz, *W* = 22.68 kg, *C* = 0.0127 cm, *L/D* = ½, *EMU* = 0.001, *FHY* = 444.8N, *ENY* = 0.5)

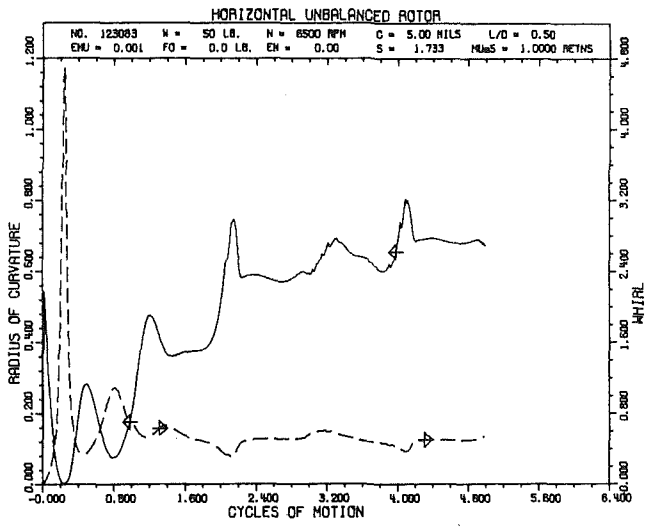

Fig. 16(*b*) Radius of curvature and whirl versus cycles of motion (*FHY* = 444.8N, *ENY* = 0.5)

gle plot clearly indicates that this assumption is not valid. One other important aspect of this plot is the fact that the phase angle is oscillating about the approximate value of 90 deg. When the phase angle does not or cannot go through a complete 180 deg inversion, large resultant forces are transmitted to the support system. Imbalance in a horizontal journal is highly undesirable and should always be reduced to the lowest possible value.

The transmissibility plots have shown the cyclic nature of the large resultant forces being transmitted to the bearing due to imbalance of the journal. This could shorten the life of the bearing surface considerably due to fatigue pitting and hence the loss of the load carrying capacity of the bearing.

The concept of whirl ratio has been derived and the plots of this quantity indicate that a constant value of whirl cannot exist in a horizontal journal (rotor), but can give the orbit the appearance of a constant whirl due to the averaging of the cyclic nature. The vertical balanced journal was the only configuration that gave a constant whirl ratio [9].

The developed program has shown the ability to predict journal orbits under various types of external cyclic loading functions and leaves no doubt as to the capability of the program to track arbitrary forcing functions. If the forcing function can be approximated by an analytic expression, then the program may be easily modified to incorporate this loading by changing a single card; otherwise a procedure will have to be added to the present program to read data cards containing values of force for each increment of time the solution will track. The latter process would present some difficulty but any arbitrary time dependent forcing function could be incorporated in the program if desired.

With the more advanced methods of data display available to researchers, the time required for the analysis of computer output has been greatly reduced. This fact permits complex systems to be simulated at a reasonable cost and within a minimum amount of time. Numerical methods that were considered impractical several years ago are now being used very effectively due to the speed and accuracy of the modern digital computers. This fact is of great importance to the practicing engineer due to the widespread availability of remote terminals which provide easy access to large time-sharing computers at a reasonable cost to the user.

References

1 Kirk, R. G., and Gunter, E. J., "Short Bearing Analysis Applied to Rotor Dynamics—Part 1 Theory," ASME Paper No. 75-Lub-30; to be published in the JOURNAL OF LUBRICATION TECHNOLOGY.

2 Sommerfeld, A., "Zur hydronamischen Theorie der Schmiermittebreibung," *Zeitschrift fur Mathematik und Phusik*, Vol. 50, 1904.

3 Radzimovsky, E. I., *Lubrication of Bearings*, The Ronald Press Company, New York, 1959.

4 Pinkus, O., and Sternlicht, B., *Theory of Hydrodynamic Lubrication*, McGraw-Hill, New York, 1961.

5 Ocvirk, F. W., "Short-Bearing Approximation for Full Journal Bearings," NACA TN 2808, 1952.

6 Hori, Y., "A Theory of Oil Whip," *Journal of Applied Mechanics*, TRANS. ASME, June 1959.

7 Hull, E. H., "Oil Whip Resonance," TRANS. ASMEa Vol. 80, 1958, pp. 1–1496.

8 Badgley, H., and Booker, J. F., "Turborotor Instability—Effect of Initial Transients on Plane Motion," Paper No. 68-Lub-7, presented at ASME-ASLE Lubrication Conference, Oct. 8–10, 1968.

9 Kirk, R. G., and Gunter, E. J., "Transient Journal Bearing Analysis," NASA CR 1549, June 1970.